Available online at www.sciencedirect.com
SCIENCE DIRECT®
Journal of Photochemistry and Photobiology A: Chemistry 158 (2003) 139–144
Journal of Photochemistry and Photobiology A:Chemistry
www.elsevier.com/locate/jphotochem

Photocatalytic activities for water decomposition of RuO_2-loaded $AInO_2$ (A = Li, Na) with d^{10} configuration

J. Sato [a], H. Kobayashi [b], N. Saito [a], H. Nishiyama [a], Y. Inoue [a,*]

[a] *Department of Chemistry, Nagaoka University of Technology, Nagaoka 940-2188, Japan*
[b] *Department of Chemistry and Bioscience, Kurashiki University of Science and the Arts, Kurashiki 712-8505, Japan*

Received 7 May 2002; received in revised form 17 July 2002; accepted 7 October 2002

Abstract

The photocatalytic activities for water decomposition of RuO_2-loaded alkaline metal indates, $AInO_2$ (A = Li, Na), with d^{10} configuration were studied. Under Hg–Xe lamp illumination, RuO_2-loaded $LiInO_2$ had little activity, but RuO_2-loaded $NaInO_2$ showed the ability to photocatalytically decompose water to hydrogen and oxygen. The photocatalytic activity strongly depended on the calcination temperature of $NaInO_2$: with increasing calcination temperature, the activity increased, passed through a maximum, and sharply decreased. In case that a part of Na ion in $NaInO_2$ was replaced by Li or K ion, the photocatalytic activity decreased sharply with a small amount of Li and gradually with increasing content of K. The calculation based on a plane wave density function theory (DFT) was employed to elucidate the band structure of $AInO_2$ (A = Li, Na). The photocatalytic activities were compared with those of previously reported RuO_2-loaded MIn_2O_4 (M = Ca, Sr), and the activity differences among them are discussed.

Keywords: Photocatalysts; Water decomposition; p-Block alkaline metal indates; d^{10} configuration

1. Introduction

In previous studies, we have reported that alkaline earth metal indates, MIn_2O_4 (M = Ca, Sr), were photocatalytically active for water decomposition to produce hydrogen and oxygen under Xe lamp illumination when RuO_2 particles were dispersed [1,2]. The other p-block metal oxides such as M_2SnO_4 (M = Ca, Sr), $NaSbO_3$, $M_2Sb_2O_7$ (M = Ca, Sr), and $ZnGa_2O_4$ have been found to be photocatalytically active for water decomposition when combined with RuO_2 [3]. Interestingly, all the core p-block metal ions of these photocatalysts have d^{10} configuration.

The conventional transition metal oxides used for photocatalysts, frequently being combined with RuO_2 or NiO as a promoter, are $SrTiO_3$ [4], $A_2Ti_6O_{13}$ (A = Na, K, Rb) [5,6], $BaTi_4O_9$ [7,8], $A_2La_2Ti_3O_{10}$ (A = K, Rb, Cs) [9,10], $Na_2Ti_3O_7$ [11], $K_2Ti_4O_9$ [12], ZrO_2 [13], $A_4Nb_6O_{17}$ (A = K, Rb) [14], $Sr_2Nb_2O_7$ [15], $ATaO_3$ (A = Na, K) [16,17], MTa_2O_6 (M = Ca, Sr, Ba) [18,19] and $Sr_2Ta_2O_7$ [15]. These transition metal oxides have a common feature that they are composed of the octahedrally coordinated metal ions with d^0 configuration. However, the photocatalytic activities were strongly dependent on the local structures of the metal oxides. $BaTi_4O_9$ and $A_2Ti_6O_{13}$ (A = Na, K, Rb) possess the tunnel structures formed by heavily distorted TiO_6 octahedra [20–22]. A model that the distorted TiO_6 octahedra play an important role in the generation of photocatalytic activity for water decomposition has been proposed.

For the development of a new series of p-block metal oxide photocatalysts, it is required to accumulate information on the electronic and local structures. Very recently, for p-block metal oxide of $Sr_2Sb_2O_7$ with d^{10} configuration, the distorted SbO_6 octahedra have been demonstrated to significantly contribute to the activity for water decomposition, indicating the important effects of local structures on the photocatalytic activity [3]. In the present study, the photocatalytic activities for water decomposition of RuO_2-loaded alkaline metal indates, $LiInO_2$, $NaInO_2$, $Na_{1-x}Li_xInO_2$, and $Na_{1-x}K_xInO_2$ were investigated. The influences of preparation conditions on the activity were examined with $NaInO_2$. To understand the electronic structures of $AInO_2$ (A = Li, Na), their band structures were calculated by using a plane wave density function theory (DFT). The photocatalytic activities were compared with those of previously reported RuO_2-loaded MIn_2O_4 (M = Ca, Sr) [1,2], and the activity differences are discussed on the basis of the local structures.

* Corresponding author. Tel.: +81-258-47-9832; fax: +81-258-47-9830.
E-mail address: inoue@analysis.nagaokaut.ac.jp (Y. Inoue).

1010-6030/03/$ – see front matter © 2003 Elsevier Science B.V. All rights reserved.
doi:10.1016/S1010-6030(03)00028-5

2. Experimental

Alkaline metal indates were prepared by a solid state reaction at high temperatures. For the synthesis of $AInO_2$ (A = Li, Na), a molar ratio mixture of In_2O_3 (Nacalai tesque, EP grade) and A_2CO_3 (A = Na, Li) (Nacalai tesque, EP grade) was calcined in air in the temperature range 1273–1573 K. For the preparations of $Na_{1-x}Li_xInO_2$ and $Na_{1-x}K_xInO_2$, the mixtures of Na_2CO_3 with Li_2CO_3 or K_2CO_3 (Nacalai tesque, EP grade) at different ratios were added instead of Na_2CO_3, respectively. The formation of the metal oxides was confirmed by X-ray diffraction patterns reported previously. The indates thus prepared were impregnated up to incipient wetness with a ruthenium carbonyl complex, $Ru_3(CO)_{12}$ (Aldrich Chemical Co., 99% pure), in tetrahydrofuran, dried at 353 K and oxidized in air at 673 K for 5 h to produce RuO_2. The amount of loaded RuO_2 was 1 wt.% as a Ru metal content.

The photocatalytic reaction was carried out in a closed gas circulating reaction apparatus. About 250 mg of powder photocatalysts was placed in a quartz reaction cell filled with ca. 30 cm^3 of distilled and ion-exchanged water. Ar gas of 13.3 kPa was circulated with a piston pump during the reaction. Powder photocatalysts were dispersed in water by stirring of Ar gas bubbling and were illuminated by a Hg–Xe lamp (Hamamatsu L5662-02) at 200 W (the wavelength range 248–365 nm) or Xe lamp (Ushio UI-501C) at 400 W (250–700 nm). The evolved gases were analyzed by an on-line gas chromatograph. The light absorption spectra of the indates were recorded on a UV reflectance spectrometer (JASCO UVIDEC-660). The DFT calculation was carried out employing the CASTEP program [23]. The core electrons were replaced by the ultra-soft core potentials. The valence electronic configurations of $NaInO_2$ are $2s^22p^63s^1$ for Na, $5s^24d^{10}5p^1$ for In and $2s^22p^4$ for O atom. The kinetic energy cutoff was taken to be 260 eV. The primitive unit cell was composed of $[NaInO_2]_2$, and the number of occupied orbitals was 34. The electronic configurations of $LiInO_2$ are the same as those of $NaInO_2$ except for $1s^22s^1$ for Li atom. The primitive unit cell was $[LiInO_2]_2$, and the number of the occupied orbitals was 28.

3. Results

Fig. 1 shows the water decomposition by RuO_2-loaded alkaline metal indates of $LiInO_2$, $NaInO_2$ and $Na_{0.9}K_{0.1}InO_2$ under Hg–Xe lamp irradiation. For $RuO_2/LiInO_2$, neither hydrogen nor oxygen was evolved in the gas phase even for long irradiation. On the other hand, in the first run of $RuO_2/NaInO_2$, hydrogen was produced in nearly proportion to irradiation time, whereas oxygen was initially fast, followed by a slow production. In the second run, the evolution of oxygen decreased and approached to a normal production level. Under Xe lamp irradiation, however, the activity of $RuO_2/NaInO_2$ was negligible. For $RuO_2/Na_{0.90}Na_{0.10}InO_2$,

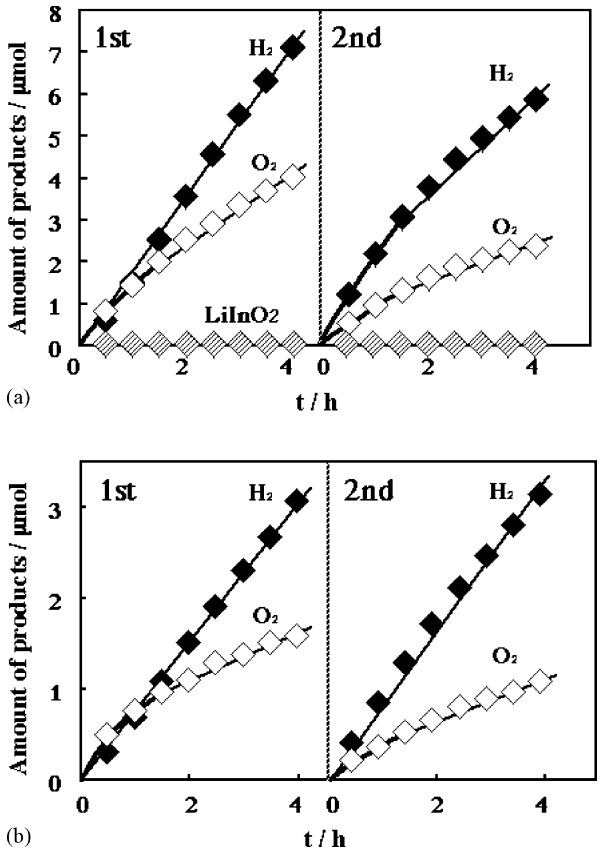

Fig. 1. Evolution of hydrogen and oxygen in photocatalytic water decomposition on RuO_2-loaded $NaInO_2$ (a) and RuO_2-loaded $RuO_2/Na_{0.90}Na_{0.10}InO_2$ (b). (◆) H_2 and (◇) O_2. The symbol ▨ in (a) represents no productions of hydrogen and oxygen from RuO_2-loaded $LiInO_2$.

the reaction behavior in the first run under Hg–Xe lamp illumination was similar to that of $RuO_2/NaInO_2$, and in the second run, H_2 and O_2 production turned to be nearly stable. No production of H_2 and O_2 was observed in the absence of RuO_2 loading.

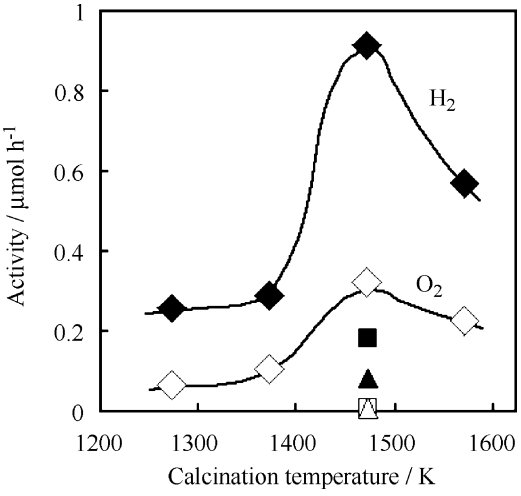

Fig. 2. Changes in activity of RuO_2-loaded $NaInO_2$ with calcination temperatures of $NaInO_2$. (◆) H_2 and (◇) O_2.

Fig. 2 shows changes in activity with the calcination temperature of $NaInO_2$. With increasing temperature, the photocatalytic activity of RuO_2-loaded $NaInO_2$ increased gradually and markedly, passed through a maximum at 1473 K and sharply decreased. Fig. 3 shows the SEM images of $NaInO_2$ calcined at different temperatures. For calcination at 1273 K, $NaInO_2$ particles had rugged shapes, and the average particle size was estimated to be 1.4 μm. At 1473 K, the shapes of the particles were nearly unchanged, but the particle size was 2.4 μm. At 1573 K, the particle size increased dramatically to 7 μm. Changes in the photocatalytic activity of $NaInO_2$ by replacing a part of Na ion by the other alkaline ions were examined. Fig. 4 shows the activity of RuO_2-loaded $Na_{1-x}A_xInO_2$ where A is Li or K ion. The activity was lowered dramatically by the addition of Li and gradually with increasing amount of K.

Fig. 5 shows the UV diffuse reflectance spectra of $LiInO_2$, $NaInO_2$, and $Na_{0.95}K_{0.05}InO_2$. For $LiInO_2$, very small light absorption began at around 440 nm. The gradual absorption continued until 350 nm, followed by a steep absorption and reached a maximum level at 290 nm. For $NaInO_2$, absorption occurred at around 430 nm and showed a bump in the wavelength range 400–350 nm, reaching a maximum level at 300 nm. For $Na_{0.95}K_{0.05}InO_2$, the pattern of absorption spectrum was analogous to that of $NaInO_2$ except for 10–20 nm shift toward longer wavelength.

Fig. 6 shows the energy-band diagram and the density of states (DOS) for $NaInO_2$ evaluated by the DFT calculation. In the DOS, the deep core band was composed of Na 2s, Na 2p, O 2s and In 4d orbitals. A broad band at valence band position was formed by the O 2p orbital. The band gap was 0.51 eV. The bottom of conduction band con-

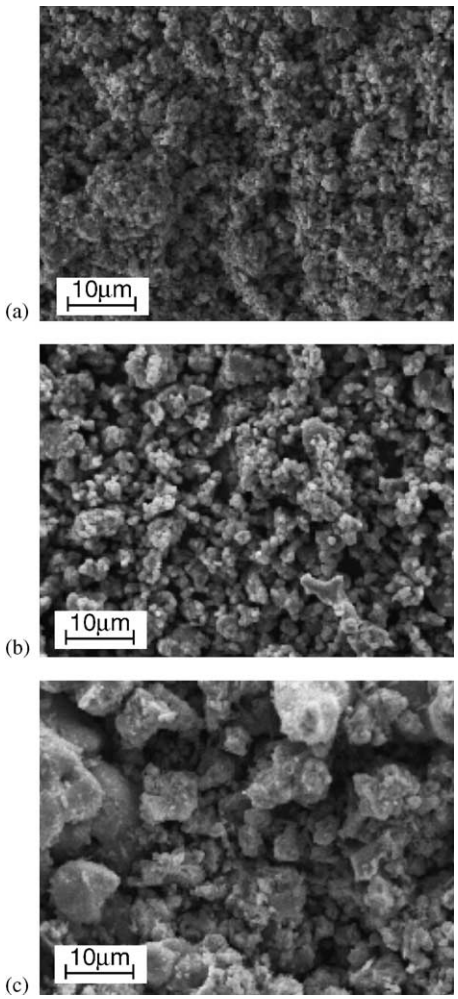

Fig. 3. SEM images of $NaInO_2$ calcined at 1273 K (a), 1473 K (b) and 1573 K (c).

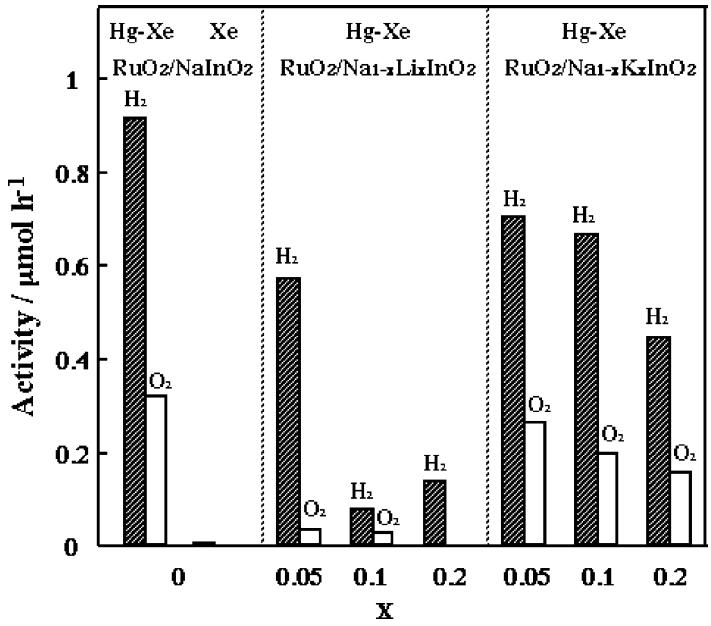

Fig. 4. Photocatalytic activities of RuO_2-loaded $Na_{1-x}A_xInO_2$ (A = Li, K). (▨) H_2 and (□) O_2.

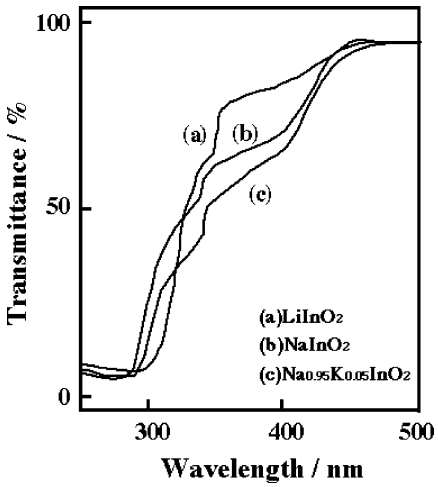

Fig. 5. UV diffuse reflectance spectra of (a) $LiInO_2$, (b) $NaInO_2$ and (c) $Na_{0.95}K_{0.05}InO_2$.

sisted of the In 5s and 5p orbitals, and Na 3s + 3p was hybridized in the upper part of the conduction band. The energy-band diagram showed large dispersion in the conduction band. In the DOS of $LiInO_2$, as shown in Fig. 7, the core levels are composed of Li 1s, O 2s, and In 4d orbitals, and the valence band was formed by the O 2p orbital. The band gap was 2.03 eV. The lower part of the conduction band consisted of the In 5s + 5p orbitals, whereas the upper part of conduction band was formed by the hybridized Li 2s + 2p orbital. $LiInO_2$ and $NaInO_2$ showed similar electronic structures. However, there was a clear difference: the band gap of $NaInO_2$ was significantly smaller than that of $LiInO_2$.

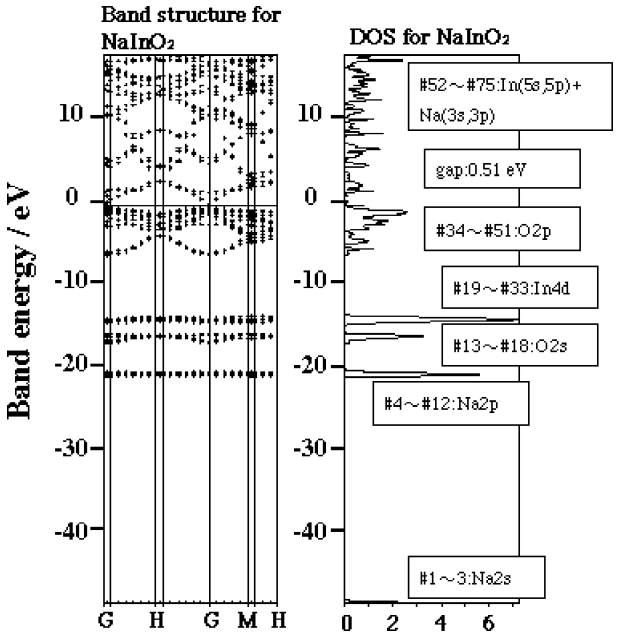

Fig. 6. Energy dispersion diagram and DOS of $NaInO_2$.

4. Discussion

The RuO_2-loaded $NaInO_2$ showed the capability to photocatalytically decompose water to produce H_2 and O_2 under Hg–Xe lamp illumination. The calcination-temperature dependence of photocatalytic activity had a maximum at an intermediate temperature of 1473 K. The appearances of a maximum in correlation between the photocatalytic activity and the calcination temperature were also observed for

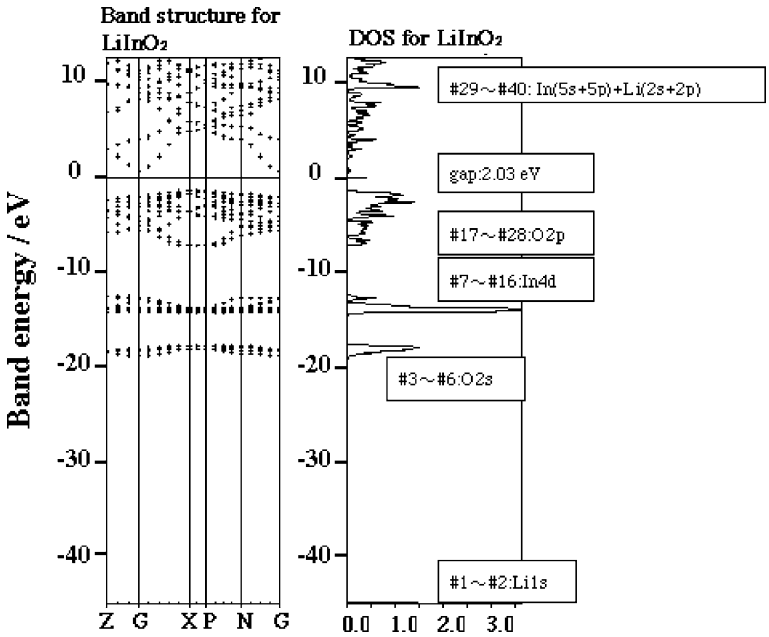

Fig. 7. Energy dispersion diagram and DOS of $LiInO_2$.

the other p-block metal oxide systems such as RuO_2-loaded $SrIn_2O_4$ [1] and RuO_2-loaded $ZnGa_2O_4$ [24]. An increase in the activity in a lower calcination temperature region is associated with the crystallization of $NaInO_2$, as is confirmed by attenuations of the full width at half maximum (FWHM) of the X-ray diffraction peaks with increasing temperature. The crystallization of $NaInO_2$ reduces the density of recombination centers due to imperfections of the crystal structures and hence raises the efficiency to produce photoexcited charges. The SEM observation showed that the average particle size of $NaInO_2$ dramatically increased by calcinations between 1473 and 1573 K. This indicates that in a higher temperature region above 1473 K, the marked growth of $NaInO_2$ particles occurred, causing a remarkable decrease in the surface area. It has been shown that the low surface area of metal oxides leads to a poor dispersion of RuO_2 particles by agglomeration [24]. Thus, a sharp drop of the activity in the higher calcination temperature above 1473 K is ascribable to decreases in the number of the active sites related to RuO_2 dispersion.

As shown in the DFT calculation, the In 4d orbitals of both $NaInO_2$ and $LiInO_2$ were located at deep core levels. The valence bands are essentially composed of the O 2p orbital in both cases. The lower part of conduction bands consisted of In 5s + 5p hybridized orbitals, whereas the upper part involved Na 3s + 3p for $NaInO_2$ and Li 2s + 2p for $LiInO_2$. The electron transfer upon illumination takes place from the O 2p to the In 5s + 5p orbitals. The large dispersion of the conduction bands exhibited the large mobility of photoexcited electrons in the bands. Thus, the electronic structures are similar between $NaInO_2$ and $LiInO_2$. However, there was a clear difference in the band gap: $NaInO_2$ provides the extremely small band gap (0.51 eV), compared to the normal band gap of $LiInO_2$ (2.03 eV). The small band gap is associated with the large overlap of the In orbitals, indicative of In–In interactions. It is likely that better photocatalytic performance of $NaInO_2$ is associated with the In–In interaction. In the UV spectra of $NaInO_2$ and $LiInO_2$, light absorption started at 400 nm and reached maximum levels at around 290–300 nm, but a difference was that only $NaInO_2$ had a bump in the wavelength region 400–360 nm. It appears that the different absorption feature reflects the differences in the calculated band gaps. It is of interest to compare the photocatalytic activities of RuO_2-loaded different kinds of the indates investigated under similar reaction conditions. Under Hg–Xe lamp irradiation, the activity was larger in the order $CaIn_2O_4$ > $SrIn_2O_4$ ≫ $NaInO_2$ ≫ $LiInO_2$. $LiInO_2$ was inactive, and the activity of $NaInO_2$ was approximately 31 and 10-fold smaller than that of $CaIn_2O_4$ and $SrIn_2O_4$, respectively [1,2]. In addition, under Xe lamp illumination, $NaInO_2$ showed little photocatalytic activity, but MIn_2O_4 (M = Ca, Sr) still reserved high photocatalytic activity. Thus, it is evident that there were intrinsic differences in the photocatalytic activity between MIn_2O_4 (M = Ca, Sr) and $AInO_2$ (A = Li, Na). The preliminary DFT calculation showed that the valence and conduction band structures for $SrIn_2O_4$ were similar to those for $NaInO_2$ [25]. Thus, the activity differences are mainly associated with local structural differences.

The photocatalytic performance of RuO_2-loaded metal oxides was determined by the dispersed states of RuO_2 and by the ability for photoexcited charge formation of the metal oxides. The structural feature of MIn_2O_4 (M = Ca, Sr) is the presence of a pentagonal prism-like tunnel structure [26]. In previous studies of photocatalytic activity of RuO_2-loaded $BaTi_4O_9$, the pentagonal prism tunnel structure of $BaTi_4O_9$ has been shown to have an advantage of accommodating RuO_2 as fine particles with the size of a few nanometer [7,8]. Thus, it is likely that MIn_2O_4 (M = Ca, Sr) have similar effects on RuO_2 dispersion. The generation of well-dispersed small RuO_2 certainly leads to high photocatalytic performance. $NaInO_2$ has a layer structure, and it is possible to produce well-dispersed RuO_2 particles on the surface, as was demonstrated for layer structural $Na_2Ti_3O_7$ and $K_2Ti_4O_9$ [11,12]. $NaInO_2$ has an advantage of the layer structure in photocatalytic performance, compared to $LiInO_2$, and there is a possibility that the structural difference is also responsible for their activity differences.

The roles of the local structures of the metal oxides are more important in photoexcited charge formation. MIn_2O_4 (M = Ca, Sr) with the pentagonal-prism-like tunnel structures are composed of two kinds of the distorted InO_6 in which respective In^{3+} is out of the center position [26]. This produces the dipole moment in the InO_6 octahedra. As shown previously, the pentagonal prism tunnel structure of $BaTi_4O_9$ is formed by two kinds of the distorted TiO_6 octahedra. The octahedra are so heavily distorted that the respective Ti^{4+} position deviates from the center of gravity of six surrounding oxygen ions, producing the dipole moment in the TiO_6 octahedra [21,22]. The model has been proposed that local electric fields due to the dipole moment promote the charge separation upon photoexcitation and hence increase the efficiency for photoexcited charge formation [27–29]. Therefore, the field effects on photoefficiency are expected with MIn_2O_4 (M = Ca, Sr). On the other hand, $AInO_2$ (A = Li, Na) have little field effects, because of the undistorted InO_6 octahedra [30,31]. This explains different photocatalytic activity between MIn_2O_4 (M = Ca, Sr) and $AInO_2$ (A = Li, Na). The present results have demonstrated that it is important to take the roles of the distorted metal-oxygen octahedral structures into account for achieving excellent photocatalytic performance.

Acknowledgements

This work was supported by CREST of JSP and by grant-in-aid for Scientific Research on Priority Area (14050044) from The Ministry of Education, Science, Sports and Culture.

References

[1] J. Sato, N. Saito, H. Nishiyama, Y. Inoue, Chem. Lett. (2001) 868–869.
[2] J. Sato, N. Saito, H. Nishiyama, Y. Inoue, J. Phys. Chem. 105 (2001) 6061–6063.
[3] J. Sato, N. Saito, H. Nishiyama, Y. Inoue, J. Photochem. Photobiol. A Chemistry 148 (2002) 85–89.
[4] K. Domen, A. Kudo, T. Onishi, J. Catal. 102 (1986) 92–98.
[5] Y. Inoue, T. Kubokawa, K. Sato, J. Phys. Chem. 95 (1991) 4059–4063.
[6] S. Ogura, M. Kohno, K. Sato, Y. Inoue, Appl. Surf. Sci. 121/123 (1997) 521–524.
[7] Y. Inoue, Y. Asai, K. Sato, J. Chem. Soc., Faraday Trans. 90 (1994) 797–802.
[8] M. Kohno, T. Kaneko, S. Ogura, K. Sato, Y. Inoue, J. Chem. Soc., Faraday Trans. 94 (1998) 89–94.
[9] T. Takata, Y. Furumi, K. Shinohara, A. Tanaka, M. Hara, J.N. Kondo, K. Domen, Chem. Mater. 9 (1997) 1063–1064.
[10] T. Takata, K. Shinohara, A. Tanaka, M. Hara, J.N. Kondo, K. Domen, J. Photochem. Photobiol. A 106 (1997) 45–49.
[11] S. Ogura, M. Kohno, K. Sato, Y. Inoue, J. Mater. Chem. 8 (1994) 2335–2337.
[12] S. Ogura, K. Sato, Y. Inoue, Phys. Chem. Chem. Phys. 2 (2000) 2449–2454.
[13] K. Sayama, H. Arakawa, J. Phys. Chem. 97 (1993) 531–533.
[14] A. Kudo, A. Tanaka, K. Domen, K. Maruya, K. Aika, T. Onishi, J. Catal. 111 (1998) 67–76.
[15] A. Kudo, H. Kato, S. Nakagawa, J. Phys. Chem. B. 104 (2000) 571–575.
[16] H. Kato, A. Kudo, Catal. Lett. 58 (1999) 153–155.
[17] T. Ishihara, H. Nishiguchi, K. Fukamachi, Y. Takita, J. Phys. Chem. B 103 (1999) 1–3.
[18] H. Kato, A. Kudo, Chem. Phys. Lett. 295 (1998) 487–492.
[19] H. Kato, A. Kudo, Chem. Lett. (1999) 1207–1208.
[20] W. Hofmeister, E. Tillmanns, W.H. Bauer, Acta Cryst. C 40 (1984) 1510–1512.
[21] D.H. Templeton, C.H. Dauben, J. Chem. Phys. 32 (1960) 1515–1518.
[22] S. Andersson, A.D. Wadsley, Acta Cryst. 15 (1962) 194–199.
[23] P.M.C. Payne, M.P. Teter, D.C. Allan, T.A. Arias, J.D. Joannopoulos, Rev. Mod. Phys. 64 (1992) 1045–1050.
[24] J. Sato, N. Saito, H. Nishiyama, Y. Inoue, J. Phys. Chem. B 106 (2002) 9048–9053.
[25] J. Sato, H. Kobayashi, N. Saito, H. Nishiyama, Y. Inoue, Unpublished data.
[26] V.R. Von Schenck, Hk. Muller-Buschbaum, Anorg. Allg. Chem. 398 (1973) 24–30.
[27] M. Kohno, S. Ogura, K. Sato, Y. Inoue, Chem. Phys. Lett. 267 (1997) 72–76.
[28] S. Ogura, M. Kohno, K. Sato, Y. Inoue, Phys. Chem. Chem. Phys. 1 (1999) 179–183.
[29] S. Ogura, M. Kohno, K. Sato, Y. Inoue, J. Chem. Soc., Faraday Trans. 93 (1997) 2433–2437.
[30] E. Hubbert-Paletta, R. Hoppe, G. Kreuzburg, Z. Anorg. Allgem. Chem. 379 (1970) 255–261.
[31] H. Glaum, S. Vogt, R. Hoppe, Z. Anorg. Allgem. Chem. 598 (1991) 129–138.